Author Manuscript

Author Manuscript

Author Manuscript

Author Manuscript

HHS Public Access

Author manuscript

Urol Oncol. Author manuscript; available in PMC 2021 February 23.

Published in final edited form as:

Urol Oncol. 2017 January ; 35(1): 30.e1–30.e8. doi:10.1016/j.urolonc.2016.07.013.

Tumor contact with prostate capsule on magnetic resonance imaging: A potential biomarker for staging and prognosis

Michael Kongnyuy, M.S.[a,1,*], **Abhinav Sidana, M.D.**[a,1], **Arvin K. George, M.D.**[a], **Akhil Muthigi, B.S.**[a], **Amogh Iyer**[a], **Richard Ho, M.D.**[a], **Raju Chelluri, M.S.**[a], **Francesca Mertan, B.S.**[b], **Thomas P. Frye, D.O.**[a], **Daniel Su, M.D.**[a], **Maria J. Merino, M.D.**[c], **Peter L. Choyke, M.D.**[b], **Bradford J. Wood, M.D.**[d], **Peter A. Pinto, M.D.**[a], **Baris Turkbey, M.D.**[b]

[a] Urologic Oncology Branch, National Cancer Institute, National Institutes of Health, Bethesda, MD

[b] Molecular Imaging Program, National Cancer Institute, National Institutes of Health, Bethesda, MD

[c] Laboratory of Pathology, National Cancer Institute, National Institutes of Health, Bethesda, MD

[d] Center for Interventional Oncology, National Cancer Institute & Clinical Center, National Institutes of Health, Bethesda, MD

Abstract

Background: The high-spatial resolution of multiparametric magnetic resonance imaging (mpMRI) has improved the detection of clinically significant prostate cancer. mpMRI characteristics (extraprostatic extension [EPE], number of lesions, etc.) may predict final pathological findings (positive lymph node [pLN] and pathological ECE [pECE]) and biochemical recurrence (BCR). Tumor contact length (TCL) on MRI, defined as the length of a lesion in contact with the prostatic capsule, is a novel marker with promising early results. We aimed to evaluate TCL as a predictor of +pathological EPE (+pEPE), +pathological LN (+pLN), and BCR in patients undergoing robotic-assisted laparoscopic radical prostatectomy.

Materials and methods: A review was performed of a prospectively maintained single-institution database of men with prostate cancer who underwent prostate mpMRI followed by robotic-assisted laparoscopic radical prostatectomy without prior therapy from 2007 to 2015. TCL was measured using T2-weighted magnetic resonance images. Logistic and Cox regression analysis were used to assess associations of clinical, imaging, and histopathological variables with pEPE, pLN, and BCR. Receiver operating characteristic curves were used to characterize and compare TCL performance with Partin tables.

Results: There were 87/379 (23.0%) +pEPE, 18/384 (4.7%) +pLN, and 33/371 (8.9%) BCR patients. Patients with adverse pathology/oncologic outcomes had longer TCL compared to those without adverse outcomes (+pEPE: 19.8 vs. 10.1 mm, $P < 0.0001$, +pLN: 38.0 vs. 11.7 mm, $P < 0.0001$, and BCR: 19.2 vs. 11.2 mm, $P = 0.001$). On multivariate analysis, TCL remained a predictor of +pEPE (odds ratio: 1.04, $P = 0.001$), +pLN (odds ratio: 1.07, $P < 0.0001$), and BCR

[*] Corresponding author. Tel.: +1-608-738-8867. speeditomike@gmail.com (M. Kongnyuy).

[1] Both the authors contributed equally.

Author Manuscript Author Manuscript Author Manuscript Author Manuscript

(hazard ratio: 1.03, $P = 0.02$). TCL thresholds for predicting +pEPE and +pLN were 12.5 and 19.7 mm, respectively. TCL alone was found to have good predictive ability for +pEPE and +PLN (pEPE: TCL_{AUC}: 0.71 vs. $Partin_{AUC}$: 0.66, $P = 0.21$; pLN:TCL_{AUC}: 0.77 vs. $Partin_{AUC}$: 0.88, $P = 0.04$).

Conclusion: We demonstrate that TCL is an independent predictor of +pEPE, +pLN, and BCR. If validated, this imaging biomarker may facilitate and inform patient counseling and decision-making.

Keywords

Biomarker; Capsule; Magnetic resonance imaging; Lymph node; Prostatic neoplasms

1. Introduction

Prostate cancer (PCa) remains the second leading cause of cancer-related deaths in men in the United States [1]. Accurate staging of PCa dictates treatment decisions and is one indication for multiparametric magnetic resonance imaging (mpMRI) [2–4]. Local staging of PCa includes assessment of extraprostatic extension (EPE), seminal vesicle involvement, and lymph node (LN) involvement, all of which guide planning of curative therapies. Current mpMRI parameters used to detect and predict final pathological EPE (pEPE), pathological LN (pLN) status, and local and biochemical recurrence (BCR) are mostly qualitative with high interreader variability owing to strong interpreter dependency and experience [5–7].

Objective mpMRI parameters with low interreader variation may predict disease outcomes. MRI-determined tumor contact length (TCL) with the prostatic capsule is an objective mpMRI-derived variable and is emerging as a stronger predictor of +pEPE [8,9]. Currently, MRI criteria to identify EPE are dependent on subjective reader visualization of the mechanical effects of macroscopic EPE, which is a relatively late development. By the time capsular bulging, periprostatic fatty tissue invasion, rectoprostatic angle obliteration, and neurovascular bundle asymmetry or involvement observed, cancer spread is likely beyond occult microscopic EPE [9]. Similarly, pretreatment evaluation of patients for LN involvement and BCR risk is limited. Lymph node evaluation is routinely dependent on size criteria on conventional computed tomography/magnetic resonance imaging (CT/MRI) [10]. Size criteria, though objective, have limited predictive value for small-to-normal-sized LNs [11]. Clinical variable–based nomograms [12–14] to predict LN staging and BCR were developed during the pre-mpMRI era, and therefore do not include novel imaging information. In this study, we aim to evaluate the association of TCL with pEPE, pLN, and BCR.

2. Methods

2.1. Patient selection

Patients were enrolled under an institutional review board–approved prospective trial (NCT00102544) at the National Cancer Institute from May 2007 to December 2015. A total of 428 patients, diagnosed with PCa, underwent robotic-assisted laparoscopic radical

Author Manuscript Author Manuscript Author Manuscript Author Manuscript

prostatectomy (RALRP). Of these, 44 patients (8, no mpMRI; 10, pre-RALRP treatment; 24, limited mpMRI [due to hip prosthesis or motion-related artifacts]; and 2, no mpMRI lesions) were excluded from the study. For the pEPE analysis, 5 additional patients were excluded owing to inconclusive evidence of +pEPE. Patients, who received any adjuvant therapy after RALRP (n = 13), were removed from the BCR analysis. Standard pelvic LN dissection involved the obturator and external iliac nodes only while extended dissection involved the obturator and iliac nodes to the aortic bifurcation.

2.2. Imaging protocol

Imaging was performed using a combination of an endorectal coil (BPX-30, Medrad) and a 16-channel cardiac surface coil (SENSE, Philips Healthcare) using a 3.0 T (Achieva, Philips Healthcare) scanner as previously described [15]. Sequences used for image interpretation comprised T1-weighted image, T2-weighted image, and diffusion-weighted image with apparent diffusion coefficient mapping, multivoxel 3D localized magnetic resonance spectroscopy, and axial 3D fast-field echodynamic contrast-enhanced MRI. Images were prospectively read by 2 experienced radiologists (B.T. and P.L.C. with prostate MRI experience of 8 and 16 years, respectively) to localize dominant prostate lesions. Suspicion for EPE on mpMRI was defined using conventional criteria of capsular obliteration, irregularity, bulging, neurovascular bundle asymmetry, or periprostatic fat extension. All included mpMRIs were reviewed to identify tumors in contact with the prostate capsule. TCL (mm) was measured (using axial T2-weighted image) by a research fellow under direct supervision of a radiologist dedicated to prostate MRI (B.T.) using the picture archiving and communication system freehand curved distance measurement tool (Fig. 1). In cases (6.2%, 24/384) where there was more than 1 lesion with capsular contact, the average of the TCLs was obtained. Lesions with no capsular contact were assigned a TCL of zero.

2.3. Data collection

Patient demographic, preoperative clinical, imaging, pathologic variables, and prostate-specific antigen (PSA) follow-up data were obtained from a prospectively maintained database built from institutional electronic records, referring physician, and outside medical records.

A single surgeon (>15-y experience) performed all RALRP procedures, and a single genitourinary pathologist (>25-y experience) reviewed all whole-mount pathology for variables such as EPE and LN status. Predicted probabilities of +pEPE and +pLN were obtained using online Partin tables [16]. Post-RALRP monitoring involved PSA testing at 1, 3, and 6 months, and yearly thereafter. BCR was defined as PSA > 0.2 ng/ml with a confirmatory value of > 0.2 ng/ml, a single PSA > 0.4 ng/ml, or receipt of salvage therapy per the guidelines of the American Urological Association of Localized Prostate Cancer Update Panel report [17].

2.4. Statistical analysis

Statistical analysis was performed using IBM SPSS (v21 Chicago, IL) and Stata version 13 (Statacorp, TX). Wilcoxon rank-sum test was used to compare differences in distribution of continuous variables, whereas the Fisher exact and Pearson Chi-square tests were used for

Author Manuscript Author Manuscript Author Manuscript Author Manuscript

categorical variables. Logistic regression was used to determine predictors of +pLN and +pEPE, and Cox regression for prediction of BCR. Receiver operating characteristics (ROC) curves were used to compare the predictive ability of TCL and Partin tables for +pEPE and +pLN. The DeLong test was used to compare ROC curves. The Youden index was used to determine TCL thresholds maximizing sensitivity and specificity for each outcome. BCR-free survival (BCRFS) was estimated using Kaplan-Meier survival analysis, and log-rank test was used to compare survival between 2 groups defined by the median TCL length (<12.2 mm vs. ≥12.2 mm) of cohort.

3. Results

A total of 415 lesions with capsular contact were identified in 384 patients with a median of 1.0 (range: 1–3) tumor per patient. Median TCL of the entire cohort was 12.2 (range: 0–65.8) mm.

3.1. pEPE analysis

Of the 428 patients who underwent RALRP, 379 were included in pEPE analysis. Demographic data, clinical, imaging, and biopsy variables of pEPE cohort are presented in Table 1. A total of 87 patients (23.0%) were with +pEPE. Patients with +pEPE were found to have a longer median TCL (19.8, range: 0–65.8 mm) compared to patients with −pEPE (10.1, range: 0–51.1 mm), $P < 0.0001$. In addition, a greater proportion of patients with +pEPE (36/87, 41.4%) had biopsy Gleason score (GS) ≥ 3 + 4 compared to patients with –pEPE (42/292, 14.4%), $P < 0.0001$. Of 132 patients with suspicion for EPE on MRI, only 37% ($n = 49$) had +pEPE, whereas 63% ($n = 83$) were negative for pEPE. The sensitivity, specificity, positive predictive value, and negative predictive values for predicting +pEPE by MRI suspicion of EPE were 56%, 72%, 37%, and 85%, respectively. Upon multivariate logistic regression analysis, increasing MRI-TCL (odds ratio [OR] = 1.04; 95% CI: 1.02–1.07; $P = 0.001$), preoperative PSA (OR = 1.04; 95% CI: 1.01–1.08; $P = 0.01$), biopsy GS sum (OR = 2.90; 95% CI: 1.56–5.39; $P < 0.0001$) and abnormal digital rectal examination (OR = 2.40; 95 CI: 1.09–5.31; $P = 0.03$) were independent predictors of +pEPE (Table 1).

ROC curves were drawn using the predicted probabilities of EPE from Partin tables and TCL. Areas under the curves (AUCs) were comparable between Partin table (0.66, 95% CI: 0.59–0.73) and TCL (0.71; 95% CI: 0.65–0.77; $P = 0.21$). The combination of TCL and PSA better predicted +pEPE compared to Partin tables [AUCs: 0.75 (not shown) vs. 0.66, $P = 0.01$]. A TCL cutoff of 12.5 mm had the highest sensitivity (77%) and specificity (59%) in predicting pEPE in our cohort (Youden index = 0.36) (Fig. 2).

3.2. pLN analysis

There were 384 (LND: 316 standard, 30 extended) men who met inclusion criteria for the pLN analysis, 18 (4.7%) of whom were +pLN. The median TCL was longer in +pLN (38.0, range: 0–65.8 mm) compared to –pLN (11.7, range: 0–51.1 mm), $P < 0.0001$. In multivariate analysis, increasing TCL (OR = 1.07; 95% CI: 1.03–1.12; $P < 0.0001$), PSA (OR = 1.06; 95% CI: 1.01–1.10; $P = 0.01$), and clinical stage >T1c (OR = 6.0; 95% CI: 1.7–21.2; $P = 0.01$) remained independent predictors of +pLN (Table 2).

Author Manuscript Author Manuscript Author Manuscript Author Manuscript

AUC of Partin table was higher than TCL alone for predicting +pLN on pathology (0.88, 95% CI: 0.81–0.96 vs. 0.77, 95% CI: 0.62–0.92, respectively), $P = 0.04$. However, combining TCL with PSA showed comparable predictive ability of +pLN compared to Partin tables (AUCs 0.84 vs. 0.88, $P = 0.170$). Compared to the TCL cutoff for +pEPE, a higher TCL cutoff of 19.7 mm was determined (with highest sensitivity of 78% and specificity of 73%: Youden index = 0.51) in predicting +pLN in our cohort (Fig. 2).

3.3. BCR analysis

A total of 371 men met inclusion criteria for BCR analysis with a median follow-up of 25.03 (range: 0.1–92.6) months. A total of 33 men (8.9%) experienced BCR during the study period, with a median estimated BCRFS of 90.4 (95% CI: 31.0–149.8) months. The median TCL for patients who experienced BCR was 19.2 (range: 0–53.2) mm compared with 11.2 (range: 0–65.8) mm for patients who did not experience BCR, $P = 0.001$. Kaplan-Meier survival analysis was used to compare BCRFS between patients with TCL less vs. more than the median (Fig. 3).

We chose the median TCL of 12.2 mm (for all 371 patients considered in the BCR analysis) for the Kaplan-Meier analysis because BCR is a time dependent analysis that does not allow us to run ROC analysis. Because the number of BCR events was low in each group, only mean estimated BCRFS could be estimated. Patients with TCL ≥ 12.2 mm had shorter mean estimated BCRFS compared to patients with TCL < 12.2 mm (62.1 ± 3.0 vs. 86.6 ± 1.6 mo, $P < 0.0001$). On Cox regression, increasing TCL (hazard ratio [HR] = 1.03; 95% CI: 1.01–1.06; $P = 0.02$), abnormal digital rectal examination (HR = 2.76; 95% CI: 1.21–6.31; $P = 0.02$), and higher biopsy GS sum (HR = 3.29; 95% CI: 1.06–6.72; $P = 0.001$) were independent predictors of BCR (Table 3).

4. Discussion

TCL, defined as length of PCa in contact with capsule, has been shown to correlate with microscopic EPE [8,9]. TCL has a good interreader reproducibility making it a promising mpMRI parameter for predicting T staging [8]. To the best of our knowledge, TCL has not been previously studied as a predictor of +pLN and BCR.

In our study, TCL emerged as an independent predictor of +pEPE with a 4% increase in risk of +pEPE per 1 mm increase in TCL. Previously, in a study of 189 radical prostatectomy patients, ultrasound-measured TCL was associated with microscopic EPE [18]. Baco et al. [9] also showed a strong correlation between MRI-TCL and pathologically measured TCL and found TCL to predict microscopic EPE on final pathology. mpMRI provides detailed anatomy of the prostate, yet assessment of EPE remains challenging. Prostate contour bulging, capsule obliteration, periprostatic fatty tissue, or neurovascular bundle asymmetry used to assess MRI EPE are limited in predicting pathological microscopic EPE [19]. This finding was confirmed in our study, where MRI EPE suspicion, based on conventional criteria, was shown to have low sensitivity and positive predictive value. Similarly, Rosenkrantz et al. [8] showed in a cohort of 98 patients who underwent mpMRI before radical prostatectomy that TCL was a stronger predictor of EPE than did subjective reader interpretations of qualitative mpMRI parameters. With continuous advancement in the

Author Manuscript Author Manuscript Author Manuscript Author Manuscript

imaging technology and radiologist experience, increasing TCL should be viewed with increased risk/suspicion for adverse whole-mount pathology.

Pelvic lymph node dissection has both prognostic/therapeutic benefit but is not without morbidity [20]. Qualitative mpMRI parameters have performed well in locoregional staging of PCa, whereas attempts at detecting or predicting nodal metastasis (based on nodal size) are limited with low sensitivity. Hovels et al. [21] in a meta-analysis looking at the diagnostic accuracy of CT/MRI in LN staging found the sensitivity/specificity of MRI to be 39%/82%, respectively. They concluded that conventional CT and MRI had limited ability to correctly identify positive nodes and should not be used for LN staging. TCL was an independent predictor of +pLN in our cohort and, as a single parameter, had moderate ability in predicting +pLN preoperatively.

Approximately 20% to 40% of patients who have undergone RALRP experience BCR [22,23], hence there is need for predictive biomarkers that can guide post-RALRP PCa management. In our analysis, TCL was one of the independent predictors of BCR, and patients with TCL greater than the median had significantly shorter BCRFS in our study. MRI suspicion scores and PIRADSv2 (recently) have been shown to be useful tools to detect and characterize PCa. High MRI suspicion [24] and PIRADS [25] scores have been shown to especially predict clinically significant PCa (GS ≥ 3 + 4). Park et al. [26] recently in a 158 patient cohort who underwent mpMRI and RALRP showed that all patients who experienced BCR (13.3%) had a PIRADS ≥ 4 indicating that mpMRI parameters can predict BCR. These parameters, however, have inherent interreader variability limiting their ability to optimally predict BCR [5,6,27]. TCL depicted from mpMRI, on the contrary, has been shown to have substantial interreader agreement [8] and could potentially optimize mpMRI's predictive capabilities for BCR. This, in turn, could help inform and guide patient counseling and treatment decisions.

The current study is the first to quantify a specific TCL threshold number for +pLN. The predictive ability of MRI-TCL alone (at the threshold cutoffs) for +pEPE and +pLN preoperatively was clinically relevant in this study, suggesting that TCL could be used as another potentially predictive tool to inform and better stratify for adverse pathology as well as patient outcome post-RALRP. Threshold TCLs for EPE prediction, reported in the literature, range from 6 to 20 mm [8,9]. Our threshold for TCL EPE falls within the range of TCLs reported in prior studies. Our study had a larger study population (370+ patients) compared to the previous studies (90 and 111 patients) and therefore should be better powered to characterize TCL's predictive and diagnostic performance.

Partin table AUC was comparable to TCL_{AUC} for +pEPE and slightly higher for +pLN. Although Baco et al. [9] have demonstrated MRI-TCL to outperform Partin tables in predicting +pEPE (TCL_{AUC} = 0.88 compared to $Partin_{AUC}$ = 0.63), no study has yet to report similar comparisons for +pLN. Modified Partin tables use predictive probabilities of a model comprising of clinical stage, PSA, and biopsy GS. In our study, TCL alone was shown to have predictive capability close to Partin tables, which highlights the strength of this parameter in predicting adverse pathology outcomes (+pEPE and +pLN), and therefore patient outcomes. Also, the predictive ability of a TCL + PSA was higher than Partin tables

Author Manuscript Author Manuscript Author Manuscript Author Manuscript

for +pEPE and comparable for +pLN. As Partin tables were validated using thousands (5,629) of patients [28], a more accurate comparison would require a larger patient population as well. Although these results are preliminary and need to be reproduced and validated, the utility of this parameter holds promise and should be considered for inclusion in predictive nomograms for PCa.

The study is not without limitations. It is a retrospective single-center study with inherent biases associated with such analysis. A prospective study with TCL measurements integrated into the imaging workflow could help validate our findings and demonstrate the clinical utility and workflow integration of MRI-TCL. Furthermore, TCL measurements were undertaken by a single reader in a center of excellence, and reproducibility of the measurements was not verified; however, interreader variability ($\kappa = 0.7$) in the measurement of TCL has previously been shown to be good compared to subjective reads of EPE ($\kappa = 0.49$) [8]. A $\kappa = 0.7$ is not great, but it is an acceptable yet improving value as radiologists continue to get better at reading MRIs. It should be noted that increased variability can have an impact on the read of TCL, as risk for adverse pathology increases per unit increase in TCL. MRI has evolved over the past 10 years of this study, which may have slightly influenced the findings. Our number of patients with adverse pathology/outcomes is small even though we reported the largest cohort of patients ($n = 384$) to date in the evaluation of TCL as a predictive tool of PCa outcomes (Baco et al., $n = 111$, Rosenkrantz et al., $n = 99$). Although the numbers are small, our study does provide the first evidence for the hypothesis that TCL predicts outcomes (pLN and BCR) after prostatectomy.

5. Conclusion

A specific TCL threshold number (mm) is reported that may have broad predictive value. TCL is an independent predictor of EPE, LN status, and BCR in patients undergoing radical prostatectomy. This objective mpMRI parameter can be easily measured and has previously been shown to have minimal interreader variability. Predictive ability of MRI-TCL is similar to Partin Tables for +pEPE and +pLN. Future validation in larger cohorts could justify TCL as a robust objective mpMRI parameter that can inform patient counseling and guide surgical planning or the need for adjuvant therapies in patients undergoing prostatectomy.

References

[1]. Siegel RL, Miller KD, Jemal A. Cancer statistics, 2016. CA: Cancer J Clin 2016;66(1):7–30. [PubMed: 26742998]

[2]. Raskolnikov D, George AK, Rais-Bahrami S, Turkbey B, Siddiqui MM, Shakir NA, et al. The role of magnetic resonance image guided prostate biopsy in stratifying men for risk of extracapsular extension at radical prostatectomy. J Urol 2015;194(1):105–11. [PubMed: 25623751]

[3]. Raskolnikov D, George AK, Rais-Bahrami S, Turkbey B, Shakir NA, Okoro C, et al. Multiparametric magnetic resonance imaging and image-guided biopsy to detect seminal vesicle invasion by prostate cancer. J Endourol 2014;28(11):1283–9. [PubMed: 25010361]

[4]. Hoeks CM, Barentsz JO, Hambrock T, Yakar D, Somford DM, Heijmink SW, et al. Prostate cancer: multiparametric MR imaging for detection, localization, and staging. Radiology 2011;261(1): 46–66. [PubMed: 21931141]

Author Manuscript Author Manuscript Author Manuscript Author Manuscript

[5]. Tay KJ, Gupta RT, Brown AF, Silverman RK, Polascik TJ. Defining the incremental utility of prostate multiparametric magnetic resonance imaging at standard and specialized read in predicting extracapsular extension of prostate cancer. Eur Urol 2015.

[6]. Ruprecht O, Weisser P, Bodelle B, Ackermann H, Vogl TJ. MRI of the prostate: interobserver agreement compared with histopathologic outcome after radical prostatectomy. Eur J Radiol 2012;81(3):456–60. [PubMed: 21354732]

[7]. Muller BG, Kaushal A, Sankineni S, Lita E, Hoang AN, George AK, et al. Multiparametric magnetic resonance imaging-transrectal ultrasound fusion-assisted biopsy for the diagnosis of local recurrence after radical prostatectomy. Urol Oncol 2015;33(10):425.e1–6.

[8]. Rosenkrantz AB, Shanbhogue AK, Wang A, Kong MX, Babb JS, Taneja SS. Length of capsular contact for diagnosing extraprostatic extension on prostate MRI: assessment at an optimal threshold. J Magn Reson Imaging 2015.

[9]. Baco E, Rud E, Vlatkovic L, Svindland A, Eggesbo HB, Hung AJ, et al. Predictive value of magnetic resonance imaging determined tumor contact length for extracapsular extension of prostate cancer. J Urol 2015;193(2):466–72. [PubMed: 25150643]

[10]. Eisenhauer EA, Therasse P, Bogaerts J, Schwartz LH, Sargent D, Ford R, et al. New response evaluation criteria in solid tumours: revised RECIST guideline (version 1.1). European journal of cancer (Oxford, England : 1990). 2009;45(2):228–47.

[11]. Giannarini G, Petralia G, Thoeny HC. Potential and limitations of diffusion-weighted magnetic resonance imaging in kidney, prostate, and bladder cancer including pelvic lymph node staging: a critical analysis of the literature. Eur Urol 2012;61(2):326–40. [PubMed: 22000497]

[12]. Stephenson AJ, Scardino PT, Eastham JA, Bianco FJ Jr., Dotan ZA, Fearn PA, et al. Preoperative nomogram predicting the 10-year probability of prostate cancer recurrence after radical prostatectomy. J Natl Cancer Inst 2006;98(10):715–7. [PubMed: 16705126]

[13]. Kattan MW, Yu C, Salomon L, Vora K, Touijer K, Guillonneau B. Development and validation of preoperative nomogram for disease recurrence within 5 years after laparoscopic radical prostatectomy for prostate cancer. Urology 2011;77(2):396–401. [PubMed: 20970840]

[14]. Han M, Partin AW, Zahurak M, Piantadosi S, Epstein JI, Walsh PC. Biochemical (prostate specific antigen) recurrence probability following radical prostatectomy for clinically localized prostate cancer. J Urol 2003;169(2):517–23. [PubMed: 12544300]

[15]. Sankineni S, George AK, Brown AM, Rais-Bahrami S, Wood BJ, Merino MJ, et al. Posterior subcapsular prostate cancer: identification with mpMRI and MRI/TRUS fusion-guided biopsy. Abdom Imaging 2015;40(7):2557–65. [PubMed: 25916869]

[16]. Institute JH-JBBU. Partin tables. Available from: http://urology.jhu.edu/prostate/partintables.php; 2012.

[17]. Cookson MS, Aus G, Burnett AL, Canby-Hagino ED, D'Amico AV, Dmochowski RR, et al. Variation in the definition of biochemical recurrence in patients treated for localized prostate cancer: the American Urological Association Prostate Guidelines for Localized Prostate Cancer Update Panel report and recommendations for a standard in the reporting of surgical outcomes. J Urol 2007;177(2):540–5. [PubMed: 17222629]

[18]. Ukimura O, Troncoso P, Ramirez EI, Babaian RJ. Prostate cancer staging: correlation between ultrasound determined tumor contact length and pathologically confirmed extraprostatic extension. J Urol 1998;159(4):1251–9. [PubMed: 9507847]

[19]. de Rooij M, Hamoen EH, Witjes JA, Barentsz JO, Rovers MM. Accuracy of magnetic resonance imaging for local staging of prostate cancer: a diagnostic meta-analysis. Eur Urol 2015.

[20]. Briganti A, Chun FK, Salonia A, Suardi N, Gallina A, Da Pozzo LF, et al. Complications and other surgical outcomes associated with extended pelvic lymphadenectomy in men with localized prostate cancer. Eur Urol 2006;50(5):1006–13. [PubMed: 16959399]

[21]. Hovels AM, Heesakkers RA, Adang EM, Jager GJ, Strum S, Hoogeveen YL, et al. The diagnostic accuracy of CT and MRI in the staging of pelvic lymph nodes in patients with prostate cancer: a meta-analysis. Clin Radiol 2008;63(4):387–95. [PubMed: 18325358]

[22]. Roehl KA, Han M, Ramos CG, Antenor JA, Catalona WJ. Cancer progression and survival rates following anatomical radical retropubic prostatectomy in 3,478 consecutive patients: long-term results. J Urol 2004;172(3):910–4. [PubMed: 15310996]

Author Manuscript Author Manuscript Author Manuscript Author Manuscript

[23]. Freedland SJ, Humphreys EB, Mangold LA, Eisenberger M, Dorey FJ, Walsh PC, et al. Risk of prostate cancer-specific mortality following biochemical recurrence after radical prostatectomy. J Am Med Assoc 2005;294(4):433–9.

[24]. Siddiqui MM, Rais-Bahrami S, Turkbey B, George AK, Rothwax J, Shakir N, et al. Comparison of MR/ultrasound fusion-guided biopsy with ultrasound-guided biopsy for the diagnosis of prostate cancer. J Am Med Assoc 2015;313(4):390–7.

[25]. Radtke JP, Boxler S, Kuru TH, Wolf MB, Alt CD, Popeneciu IV, et al. Improved detection of anterior fibromuscular stroma and transition zone prostate cancer using biparametric and multiparametric MRI with MRI-targeted biopsy and MRI-US fusion guidance. Prostate Cancer Prostatic Dis 2015;18(3):288–96. [PubMed: 26078202]

[26]. Park JJ, Kim CK, Park SY, Park BK, Lee HM, Cho SW. Prostate cancer: role of pretreatment multiparametric 3-T MRI in predicting biochemical recurrence after radical prostatectomy. AJR Am J Roentgenol 2014;202(5):W459–65. [PubMed: 24758681]

[27]. Muller BG, Shih JH, Sankineni S, Marko J, Rais-Bahrami S, George AK, et al. Prostate cancer: interobserver agreement and accuracy with the revised prostate imaging reporting and data system at multiparametric MR imaging. Radiology 2015;277(3):741–50. [PubMed: 26098458]

[28]. Eifler JB, Feng Z, Lin BM, Partin MT, Humphreys EB, Han M, et al. An updated prostate cancer staging nomogram (Partin tables) based on cases from 2006 to 2011. BJU Int 2013;111(1):22–9. [PubMed: 22834909]

Author Manuscript Author Manuscript Author Manuscript Author Manuscript

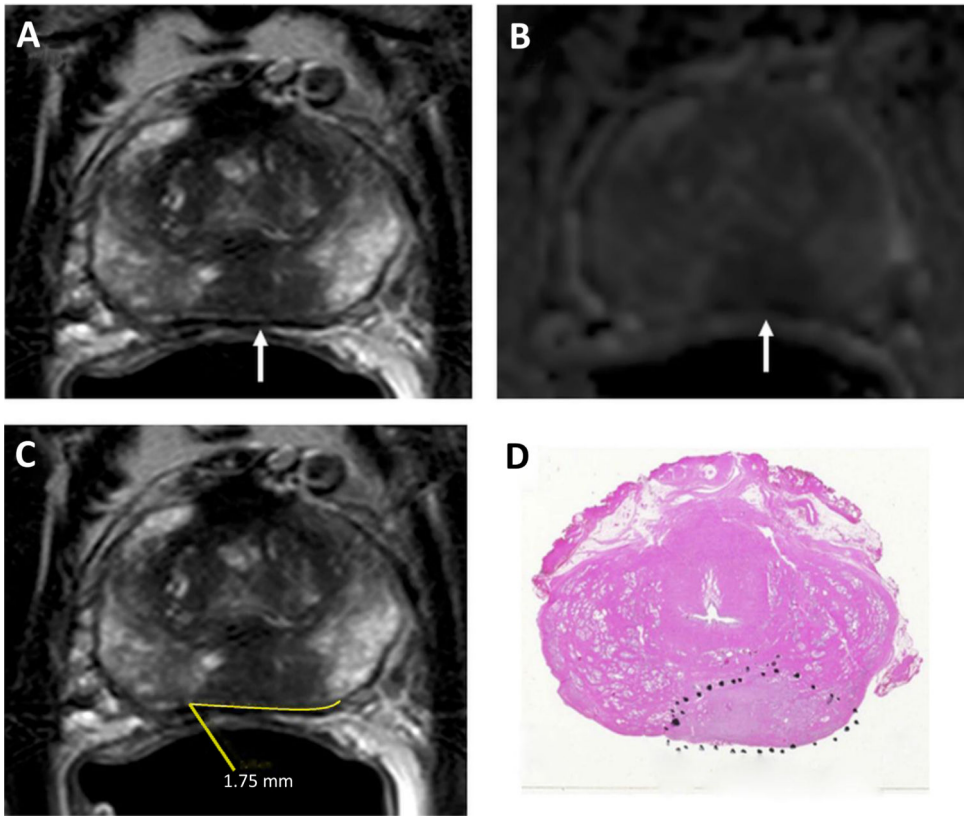

Fig. 1.

A 53-year-old man with a serum PSA = 23.70 ng/ml. Axial T2W MRI (A) and ADC map of DW MRI (B) show a midline to the left peripheral zone lesion (arrows), which represents a Gleason 3 + 4 prostate cancer lesion detected on TRUS-guided systematic prostate biopsy. The lesion does not have an overt extension but has a TCL of 17.5 mm (= 1.75 cm) measured on axial T2W MRI (C). Whole-mount prostatectomy specimen with H&E staining shows Gleason 4 + 4 prostate cancer within the lesion and posterior extraprostatic extension (inked in black) (D).

Author Manuscript Author Manuscript Author Manuscript Author Manuscript

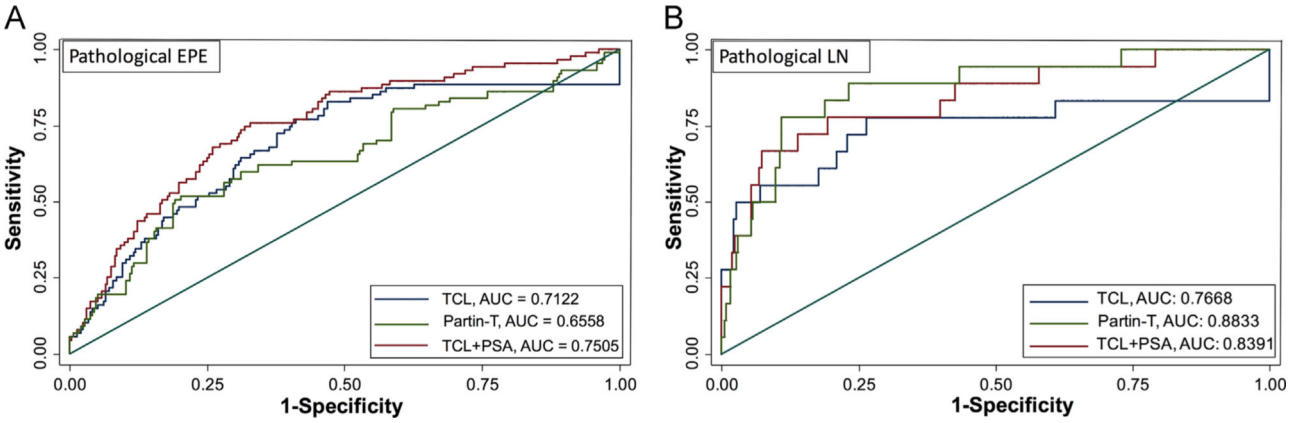

Fig. 2.

Receiver operating characteristics (ROCs) curves and areas under the curves (AUCs) of Partin tables (Partin-T), magnetic resonance image–determined tumor contact length (MRI-TCL), and MRI-TCL + PSA to predict the presence of pathological extraprostatic extension (EPE) (A) and presence of pathological lymph node (LN) involvement (B).

Author Manuscript Author Manuscript Author Manuscript Author Manuscript

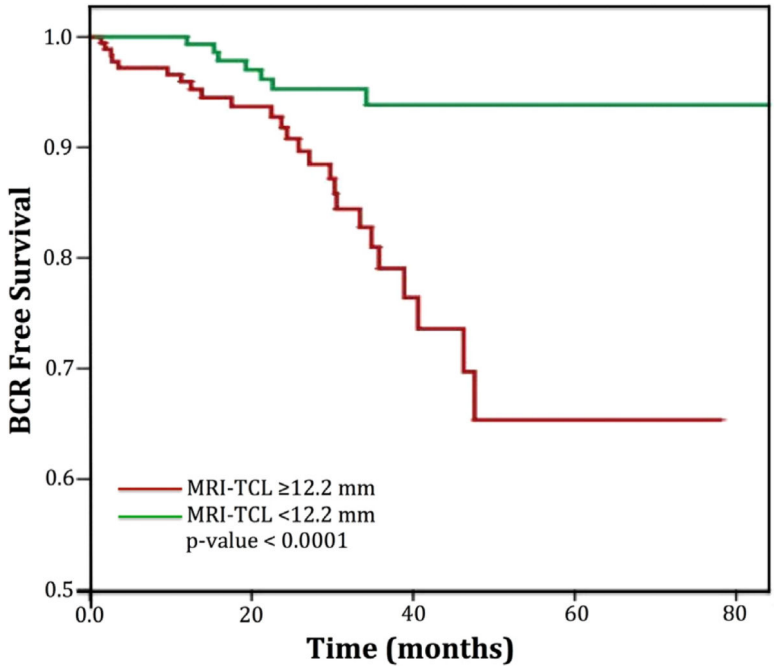

Fig. 3.

Kaplan-Meir curves showing biochemical recurrence (BCR)–free survival between 2 groups of patients separated by the median tumor contact length (12.2 mm) of BCR cohort.

Author Manuscript Author Manuscript Author Manuscript Author Manuscript

Table 1

Patient demographics as well as logistic regression analysis of predictive variables of pathological extraprostatic extension (pEPE)

Characteristics, pathologic EPE, *N* = 379	+pEPE, *n* = 87	−pEPE, *n* = 292	Univariate *P* values	Multivariate OR (95% CI)	*P* values
Median age, y (range)	61.0 (47–75)	60.0 (38–76)	**0.04**	1.01 (0.97–1.06)	0.60
Median PSA, ng/ml (range)	8.8 (0.2–53.5)	5.5 (0.1–55.7)	**<0.0001**	1.04 (1.01–1.08)	**0.01**
Clinical stage, DRE (%)					
T1C	70 (80.5)	269 (92.1)	–		
≥T2A	17 (19.5)	23 (7.9)	**0.003**	2.40 (1.09–5.31)	**0.03**
Race (%)					
White	67 (81.7)	210 (73.7)	–		
Black	10 (12.2)	61 (21.4)	0.07	0.48 (0.20–1.13)	0.09
Other	5 (6.1)	14 (4.9)	0.83	1.01 (0.27–3.74)	0.99
Median MRI-TCL, mm (range)	19.8 (0–65.8)	10.1 (0–51.1)	**<0.0001**	1.04 (1.02–1.07)	**0.001**
Biopsy GS distribution (%)					
GS sum 6 and 7	51 (58.6)	250 (85.6)	–		
GS sum ≥8	36 (41.4)	42 (14.4)	**<0.0001**	3.12 (1.65–5.92)	**<0.0001**
Median MRI prostate volume, cm^3 (range)	34.0 (15.0–135.4)	37.0 (16.0–158)	0.87		
MRI suspicion score (%)					
Low and low-moderate	5 (5.7)	42 (14.4)	–	–	
Moderate	29 (33.3)	160 (55.0)	0.41	1.0 (0.34–2.9)	1.0
Moderate-high and high	53 (60.9)	89 (30.6)	**0.001**	1.69 (0.57–5.03)	0.35

DRE = digital rectal examination.

Urol Oncol. Author manuscript; available in PMC 2021 February 23.

Author Manuscript Author Manuscript Author Manuscript Author Manuscript

Table 2

Patient demographics as well as logistic regression analysis of predictive variables of pathological lymph node involvement (pLN)

Characteristics, pathologic pLN, *N* = 384	+pLN, *n* = 18	−pLN, *n* = 366	Univariate *P* values	Multivariate OR (95% CI)	*P* values
Median age, y (range)	61 (50–72)	60 (38–76)	0.27		
Median PSA, ng/ml (range)	14.7 (1.2–53.5)	5.6 (0.1–55.7)	**<0.0001**	1.06 (1.01–1.10)	**0.01**
Clinical stage, DRE (%)					
T1C	12 (66.7)	331 (90.4)	–		
≥T2A	6 (33.3)	35 (9.6)	**0.003**	6.0 (1.7–21.2)	**0.01**
Race (%)					
White	12 (70.6)	267 (75.2)	–		
Black	4 (23.5)	70 (19.7)	0.69		
Other	1 (5.9)	18 (5.1)	0.84		
Median MRI-TCL, mm (range)	38.0 (0–65.8)	11.7 (0–51.1)	**<0.0001**	1.07 (1.03–1.12)	**<0.0001**
Biopsy GS distribution (%)					
GS sum 6 and 7	9 (50)	296 (80.9)	–		
GS sum ≥8	9 (50)	70 (19.1)	**0.003**	2.40 (0.76–7.53), 0.14	
Median MRI prostate volume, cm^3, (range)	40.1 (15–133)	36.8 (15–158)	0.08	1.01 (0.99–1.04), 0.34	
MRI suspicion score (%)					
Low and low-moderate	0 (0)	47 (12.9)	–		
Moderate	3 (16.7)	189 (51.8)	0.99		
Moderate-high and high	15 (83.3)	129 (35.3)	0.99		

DRE = digital rectal examination.

Urol Oncol. Author manuscript; available in PMC 2021 February 23.

Author Manuscript Author Manuscript Author Manuscript Author Manuscript

Table 3

Variable description and Cox proportional regression analysis results for prediction of biochemical recurrence

Characteristics pathologic BCR, *N* = 371	BCR (*n* = 33)	No BCR (*n* = 338)	Univariate *P* value	Multivariate HR (95% CI)	*P* value
Median age at RARP, y (range)	57 (46–73)	60 (38–76)	0.26		
Median pre-OP PSA, ng/ml (range)	8.9 (0.6–46.0)	5.5 (0.1–55.7)	**0.03**	1.02 (0.99–1.05)	0.31
Clinical Stage, DRE (%)					
T1C	24 (72.7)	309 (91.4)	–		
≥T2A	9 (27.3)	29 (8.6)	**0.003**	2.76 (1.21–6.31)	**0.02**
Race (%)					
White	23 (74.2)	245 (74.7)	–		
Black	5 (16.1)	67 (20.4)	0.43		
Other	3 (9.7)	16 (4.9)	0.45		
Median MRI-TCL, mm (range)	19.2 (0–53.2)	11.2 (0–65.8)	**0.001**	1.03 (1.01–1.06)	**0.02**
Biopsy GS distribution (%)					
GS sum 6 and 7	19 (57.6)	279 (82.5)	–		
GS sum ≥8	14 (42.4)	59 (17.5)	**<0.0001**	3.29 (1.61–6.72)	**0.001**
Median MRI prostate volume cm^3 (range)	30.2 (20–93)	37.0 (15–158)	0.12		
MRI Suspicion score (%)					
Low and low-moderate	0(0)	46 (13.6)	–		
Moderate	9 (27.3)	180 (53.4)	0.90		
Moderate-high and high	24 (72.7)	111 (32.9)	0.89		

DRE = digital rectal examination; RARP = robotic-assisted radical prostatectomy.

Urol Oncol. Author manuscript; available in PMC 2021 February 23.